JOURNAL OF MATERIALS SCIENCE 17 (1982) 1903–1914

The microstructure and deformation of model ABS compounds

Part 2 *The effect of graft frequency and rubber particle size*

M. DILLON*, M. BEVIS
Department of Non-Metallic Materials, Brunel University, Uxbridge, Middlesex, UK

Model ABS compounds have been used to investigate the effect of graft frequency and rubber particle size on microstructure and mechanical properties. Graft frequency was found to have a marked effect on the microstructure of ABS polymers and increasing the graft frequency resulted in an improvement in the dispersion of the rubber phase.

1. Introduction

Part 1 [1] described the techniques of electron microscopy and tensile testing and their application to the investigation of the effect of matrix molecular weight and rubber content on the microstructure and properties of model ABS compounds. The aim of the work described in this paper was to use the same techniques to investigate the effect of rubber particle size and graft frequency for a series of model compounds containing 15 per cent by weight of rubber.

2. Study materials

Four groups of ABS materials were examined, coded I to IV in order of increasing particle size, with each group comprising a well defined particle size and five degrees of grafting, as indicated in Part 1 [1], and as listed in Table I.

Specimens for tensile testing and microstructural characterization were prepared and then examined using the methods described in Part 1 [1].

3. Experimental results

3.1. Microstructure

The microstructures of the model graft materials were studied in ultramicrotomed sections using the transmission electron microscope (TEM). Typical microstructures of ABS–I specimens, containing an average particle size of 0.12 μm, are shown in Fig. 1. The effect of increasing graft frequency was observed to influence the distribution of the rubber phase. At low graft frequencies the rubber particles were strongly agglomerated and the uniformity of distribution of the included phase improved with increasing graft frequency. Higher magnification transmission electron micro-

TABLE I Graft characteristics of model ABS systems used

ABS	Average particle diameter (μm)	Measured graft frequency*	Graft degree
Ia	0.12	12	0.08
b		41	0.27
c		51	0.33
d		54	0.35
e		75	0.48
IIa	0.16	60	0.25
b		72	0.31
c		83	0.35
d		90	0.38
e		90	0.38
IIIa	0.26	76	0.20
b		105	0.27
c		126	0.33
d		169	0.45
e		195	0.51
IVa	0.4	352	0.60
b		419	0.71
c		456	0.78
d		516	0.88
e		536	0.92

*Graft frequency is measured in grains of SAN per μm^2 of particle surface $\times 10^{-16}$.

*Present address: Wavin Plastics Ltd, Durham, UK.

0022–2461/82/071903–12$03.94/0

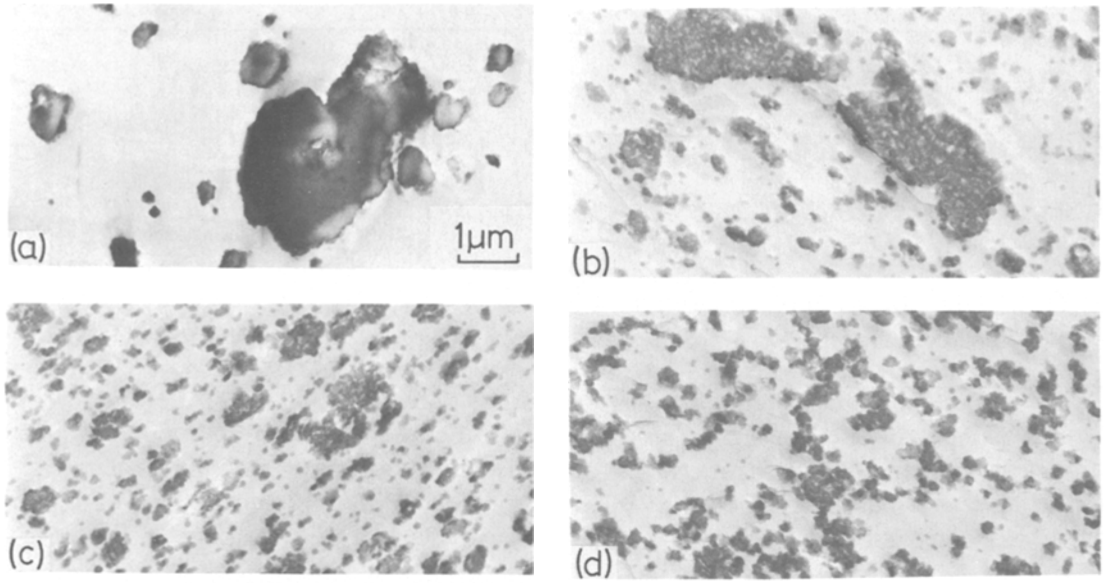

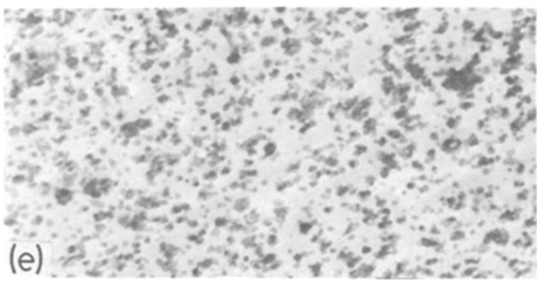

Figure 1 Transmission electron micrographs of ABS–Ia to ABS–Ie polymers respectively.

graphs of ABS–I materials are shown in Fig. 2. The rubber particles in ABS–Ia specimens (low graft) have coalesced to form continuous areas of rubber with little indication of individual particles. Increasing the graft frequency reduced the extent of agglomeration and individual particles were clearly resolved within the agglomerated regions. The effect of increasing graft frequency was therefore to improve the distribution of elastomeric inclusions. This effect was also observed for ABS–II materials, containing an average particle size of 0.16 μm (Fig. 3).

Typical transmission electron micrographs of the microstructure of ABS–III polymers (average particle size = 0.26 μm) are shown in Fig. 4. Increasing graft frequency resulted in an improved distribution of rubber particles in a similar manner to ABS–I and ABS–II materials. Additionally, the higher magnification studies of ABS–IIIa and ABS–IIIe specimens, with low and high graft frequencies respectively, indicated that increasing graft frequency caused a small increase in occluded SAN.

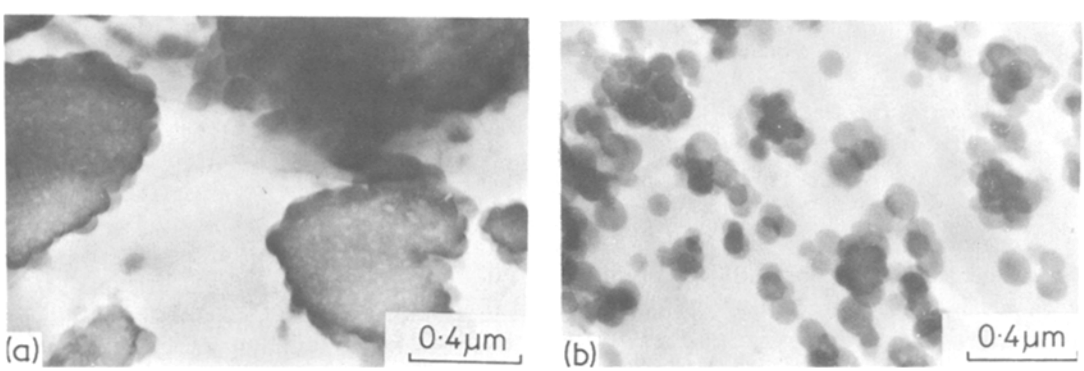

Figure 2 High magnification transmission electron micrographs of a microtomed section of (a) ABS–Ia (low graft frequency) and (b) ABS–Ie (high graft frequency).

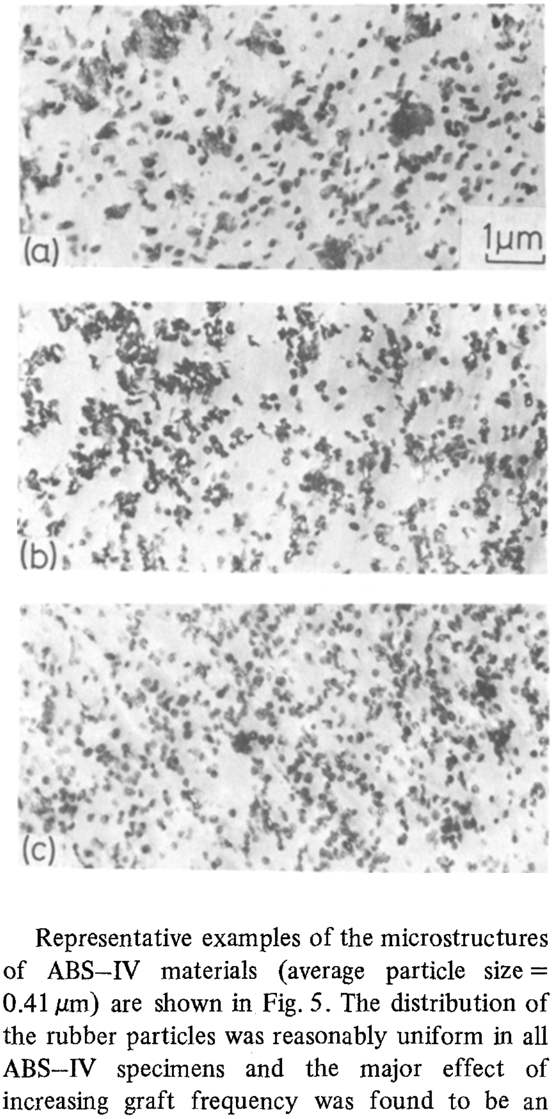

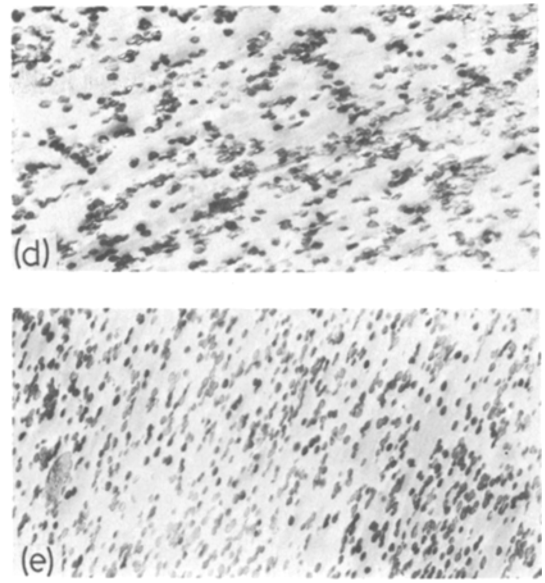

Figure 3 Transmission electron micrographs of ABS–IIa and ABS–IIe polymers respectively.

Representative examples of the microstructures of ABS–IV materials (average particle size = 0.41 μm) are shown in Fig. 5. The distribution of the rubber particles was reasonably uniform in all ABS–IV specimens and the major effect of increasing graft frequency was found to be an increase in the amount of occluded SAN. This effect is shown in more detail in Fig. 6. For ABS–IVe specimens, which contained the highest graft frequency of the series, the dispersion of rubber was found to be irregular with dense areas and depleted areas of rubber particles. Since this structure was not consistent with the general trend of ABS–IV materials it was attributed to inefficient blending of ABS and SAN resins and not a consequence of grafting. However, the micromorphology of individual rubber particles was in agreement with the observed trend and contained an increased amount of occluded SAN compared with materials of lower graft frequency.

The overall effects of increasing graft level in controlling the dispersion and microstructure of the rubber phase observed in the present investigation were in good agreement with the results of a similar study by Stabenow and Haff [2].

3.2. Mechanical properties

Due to the small amount of material available, only five specimens of each grade were tested, although there was little variation in the tensile behaviour of specimens of the same grade. The tensile properties were characterised by plotting stress–strain curves of materials with low and high graft frequencies and comparing the effect of increasing graft frequency on the yield stress and strain to failure of specimens of each series.

The tensile data for ABS–I series, containing an average particle size of 0.11 μm, are shown in Fig. 7. All materials exhibited yielding and associated stress whitening although differences in stress whitening behaviour were recorded. ABS–Ia specimens, which were found to contain large areas of strongly agglomerated rubber particles, stress whitened over the entire gauge length on yielding and the stress–strain curve did not experience a drop in stress. In contrast, ABS–I materials with increased graft frequencies tended to stress whiten at localised areas along the gauge length and these areas expanded and coalesced with increasing strain. This localisation of stress whitening gave rise to a significant drop in stress after yielding and the extent of the

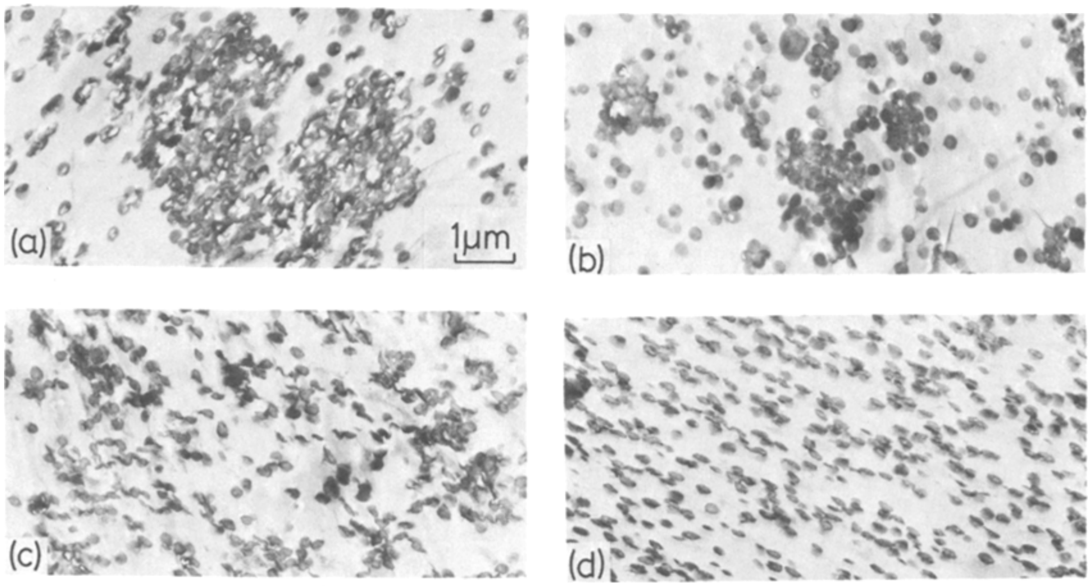

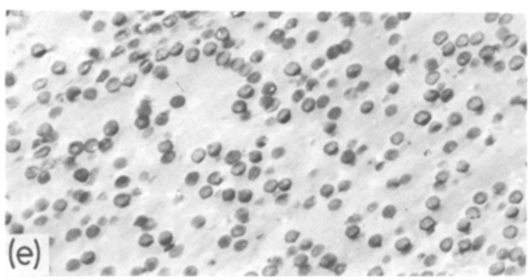

Figure 4 Transmission electron micrographs of ABS–IIIa and ABS–IIIe polymers respectively.

decrease in stress increased with increasing graft frequency. The overall effect of increasing graft frequency on the mechanical properties was an increase in both yield stress and strain to failure. Similar trends were also observed for ABS–II and ABS–III materials, which essentially contained solid rubber inclusions, shown in Figs 8 and 9.

The mechanical properties of ABS–IV materials, with an average rubber particle size of 0.41 μm are shown in Fig. 10. The anomalous microstructure observed in ABS–IVe specimens (Fig. 7) resulted in a considerable reduction in tensile properties and the stress–strain curve of this grade of ABS was very similar to the stress–strain curve of ABS–Ia. The reduced mechanical properties of ABS–IVe specimens were related to the poor distribution of the elastomeric phase which resulted from inefficient blending of SAN and ABS resins and consequently this result will not be considered further. The strain to failure for specimens of ABS–IVa to ABS–IVd did not vary significantly and the effect of increasing graft frequency was found to be a reduction in yield stress and post-yield stress. In contrast to ABS model materials containing solid rubber inclusions, the post-yield deformation of ABS–IV materials occurred at an almost constant value of stress.

3.3. Deformation

Ultramicrotomed sections prepared from stress whitened areas adjacent to the fracture surface of specimens of each series were examined in the TEM. Typical deformation structures of ABS–I polymers are shown in Fig. 11. All specimens revealed clear evidence of crazing and the craze traces exhibited a dark contrast, identical in nature to previous observations of crazes in ultramicrotomed sections. For specimens with low graft frequencies, coarse crazes emanated from the rubber agglomerations into rubber depleted areas and in many instances large voids were observed within the agglomeration. The improved dispersion of rubber particles in the highly grafted materials led to a more uniform distribution of fine crazes. Examination of deformed solvent cast films in the TEM suggested that craze formation in specimens with low graft frequencies was accompanied by voiding at the rubber inclusion–craze interface. An example of this is shown in Fig. 12.

The microstructures observed in thin sections prepared from stress whitened regions of ABS–II

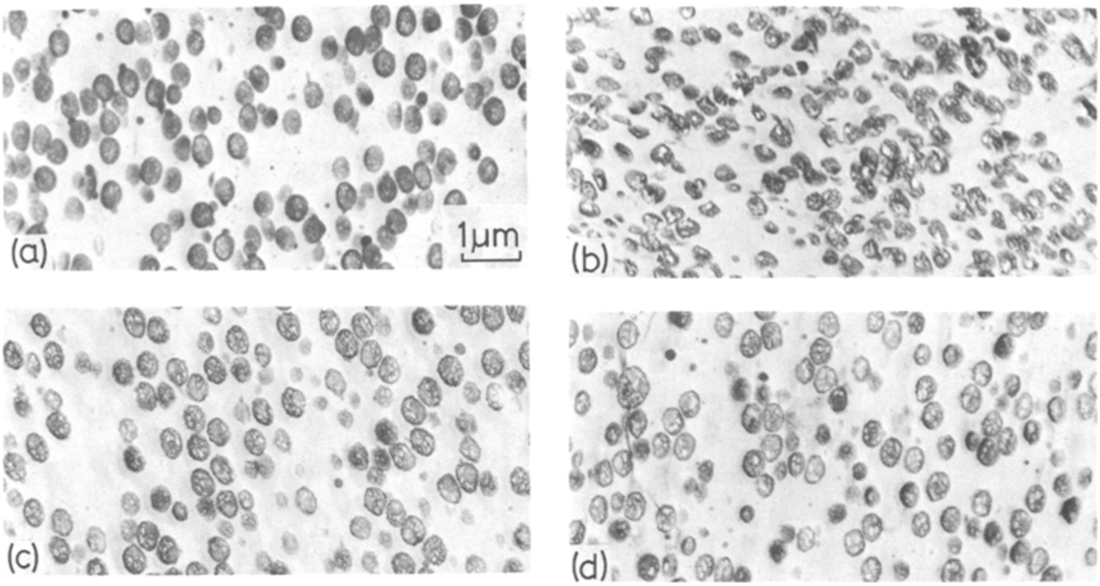

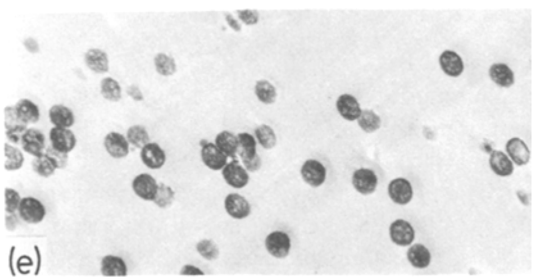

Figure 5 Transmission electron micrographs of ABS–IVa and ABS–IVe polymers respectively.

and ABS–III specimens were essentially the same as those in ABS–I specimens, and materials with increased graft frequencies were found to contain a more uniform distribution of crazes which was associated with the improved dispersion of the elastomer phase.

All grades of ABS–IV materials contained a reasonably uniform dispersion of rubber particles and the effect of increasing graft frequency was found to be an increase in occluded SAN. This increase in occluded SAN resulted in substantial differences in the deformation morphologies of bulk specimens. Typical transmission electron micrographs of ultramicrotomed sections of ABS–IVa and ABS–IVd are shown in Fig. 13. ABS–IVa exhibited a large number of coarse crazes which formed predominantly normal to the tensile axis. The lateral growth of crazes was clearly restricted by the large rubber inclusions

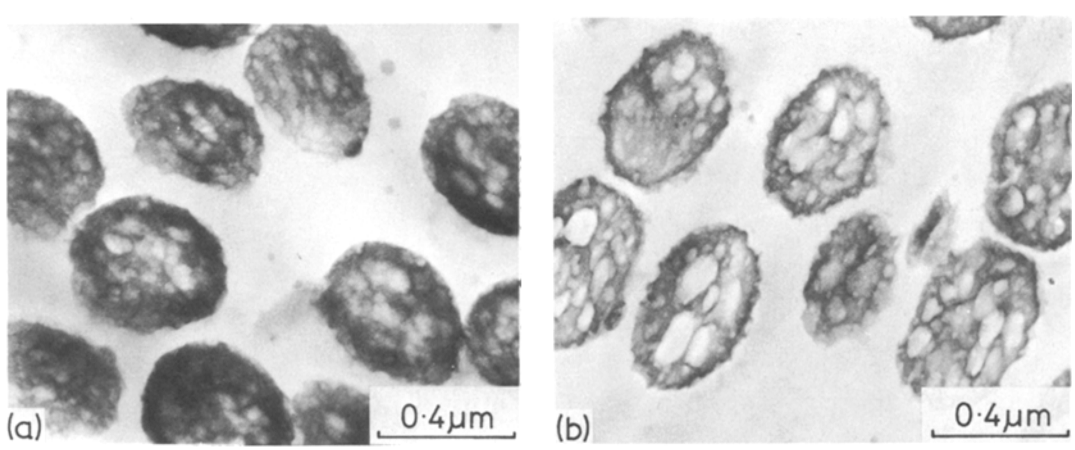

Figure 6 Details of (a) ABS–IVa (low graft frequency), showing uniformly dispersed rubber particles and small amounts of occluded SAN, and (b) ABS–IVd (high graft frequency) showing an increased frequency of occluded SAN.

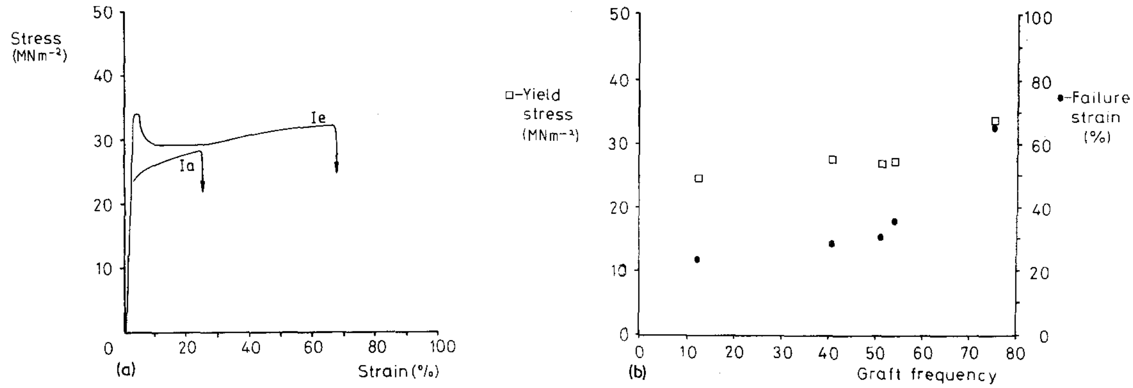

Figure 7 (a) Stress–strain curves of ABS–Ia and ABS–Ie and (b) a plot of fracture stress and strain to failure against graft frequency for ABS–I polymers. Graft frequency in grams of SAN per μm^2 of particle surface $\times 10^{-16}$.

to an extent that in many cases craze propagation was seen to be effectively terminated. Additionally the rubber particles were found to be oriented in a direction parallel to the tensile axis which indicated that craze formation was accompanied by cold drawing of the matrix material. In contrast, inclusions in ABS–IVd specimens showed no evidence of orientation but there was a significant increase in the number of crazes emanating from the rubber particles. Crazes which formed away from the equators of the inclusions were curvilinear. These differences in deformation micromorphology were also observed in solvent cast films and typical examples are shown in Fig. 14. For ABS–IVa specimens, crazes formed essentially at the equators of the rubber particles, whereas for ABS–IVd specimens, which contained an increased fraction of occluded SAN, crazes formed at a number of sites along the rubber particle circumference. The variations in contrast occurring within the deformed rubber particles of ABS–IVd further illustrated the complex deformation behaviour of inclusions containing large amounts of SAN.

3.4. Fracture

Fracture surfaces of ABS–I and ABS–IV specimens were examined in detail in the SEM. The fracture surface of ABS–Ia specimens did not contain a well defined region of slow crack growth but an initiation site of fracture was identified. High magnification studies of this area revealed a large number of voids, approximately 0.5 to 1 μm in diameter, which indicated that crack initiation was associated with the breakdown of agglomerated rubber particles. A typical example of the fracture initiation region of a specimen of ABS–Ia is shown in Fig. 15a. Well defined regions of slow and fast crack growth were apparent in specimens with increased graft frequencies. An example of

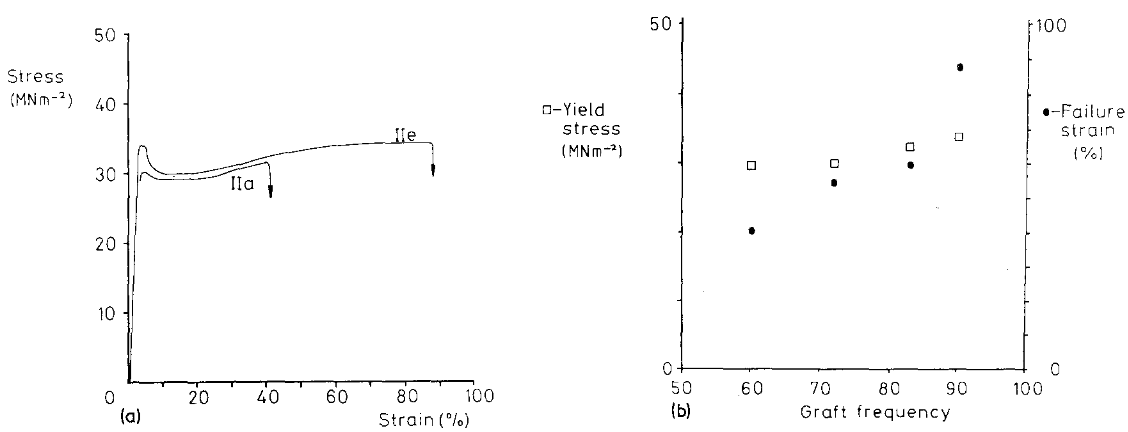

Figure 8 (a) Stress–strain curves of ABS–IIa and IIe and (b) plot of fracture stress and strain to failure against graft frequency for ABS–II polymers.

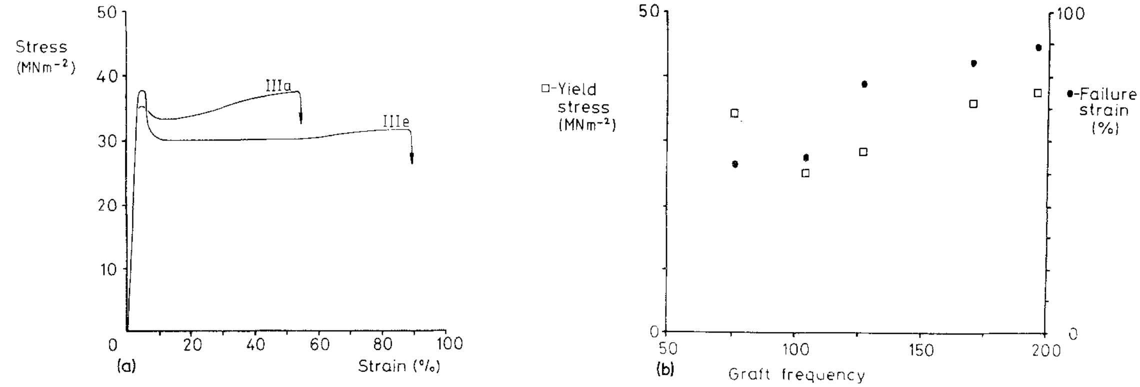

Figure 9 (a) Stress–strain curves of ABS–IIIa and ABS–IIIe and (b) plot of fracture stress and strain to failure against graft frequency for ABS–III polymers.

the slow crack growth region of a specimen of ABS–Ia is shown in Fig. 15b. This region contained a highly drawn morphology and there was little indication of rubber particles.

The fracture surfaces of ABS–IV materials were very similar and all specimens exhibited features typical of two stage ductile fracture, i.e. slow and fast crack growth regions. Representative scanning electron micrographs of the slow crack growth region of specimens of ABS–IVa and ABS–IVd are shown in Fig. 16. The fine structural details of this region were also similar and all specimens exhibited a highly drawn micromorphology.

4. Discussion

The effect of graft frequency on the microstructure of ABS was most noticeable in materials containing small, solid rubber particles, i.e. ABS–I and ABS–II series (Figs 1 and 3). On examining ultra-thin specimens of these materials in the TEM it was clearly apparent that increasing the graft frequency resulted in an improvement in the distribution of the elastomer phase. At low graft frequencies, the rubber phase consisted of large agglomerated areas, and in the case of ABS–Ia, there was little evidence of discrete rubber particles within these regions. By increasing the graft frequency, individual rubber particles became more evident to an extent that materials with the highest graft frequency of each series were found to contain a uniform dispersion of particles. These observations are consistent with the view by Huguet and Paxton [3] that the grafted SAN forms a shell around the rubber particles and thereby prevents agglomeration in ABS polymers. In a series of experiments on two polybutadiene lattices, with different particle size, these authors indicated that a shell of SAN approximately 0.01 μm thick was necessary to prevent such agglomerations.

For ABS–III materials, containing an average particle diameter of 0.26 μm the effect of increasing the graft frequency was also found to improve

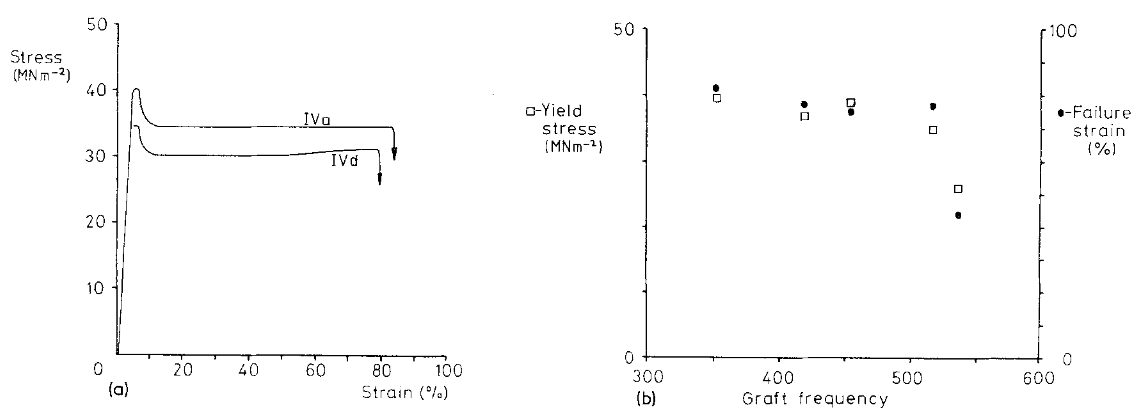

Figure 10 (a) Stress–strain curves of ABS–IVa and ABS–IVd and (b) plot of fracture stress and strain to failure against graft frequency for ABS–IV polymers.

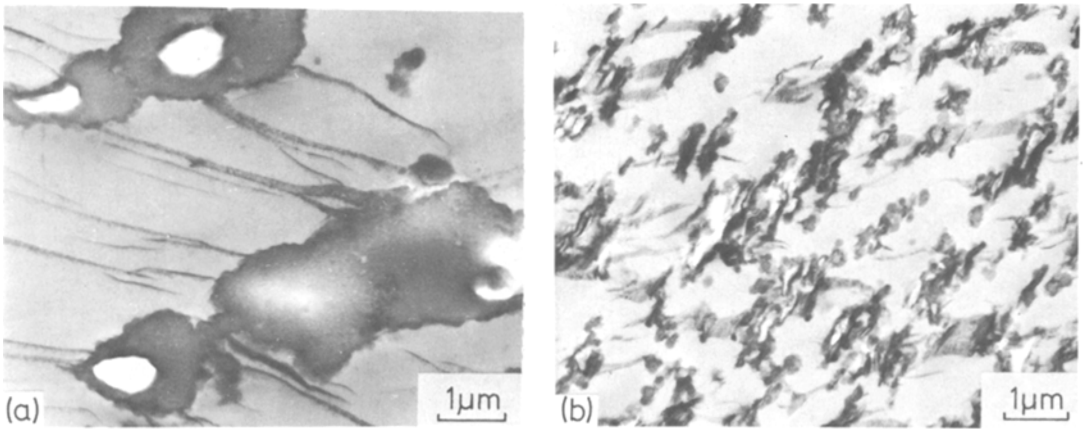

Figure 11 Typical transmission electron micrographs of microtomed sections prepared from stress whitened areas of (a) ABS–Ia and (b) ABS–Ie.

the dispersion of the included phase. Additionally, higher magnification observations of specimens of ABS–IIIe (high graft frequency) indicated that small amounts of SAN were occluded in the rubber particles.

The rubber phase in ABS–IVa and ABS–IVd specimens (average particle diameter = 0.41 μm) was uniformly dispersed which suggests that there was sufficient grafted SAN on the particle surfaces to prevent agglomerations. ABS–IVe specimens, with the highest graft frequency of the series, were found to contain an irregular dispersion of rubber particles, but this was considered to be an anomalous microstructure resulting from inefficient blending rather than a consequence of grafting and was therefore untypical of the overall trend. The effect of increasing the graft frequency was observed to be an increase in occluded SAN. Stabenow and Haff [2] have indicated that when the matrix material is present within the rubber it is difficult to distinguish between grafted and ungrafted material by normal chemical methods since the solvent extraction technique, used in the first stage of analysis to separate grafted polymer plus rubber from ungrafted polymer, is less efficient when the polymer is occluded. Presumably then, the measured values of graft frequency, listed in Table I, of specimens containing occluded SAN will contain a contribution from such ungrafted SAN. Therefore it becomes difficult to relate microstructure, and hence mechanical properties, directly with grafting. However, the study of deformation in ultramicrotomed sections and cast films gave no indication of poor adhesion between the occlusions and rubber particles, which might be expected if the occluded SAN was largely ungrafted, and consequently it is considered reasonable to assume that the effect of ungrafted SAN, if any, is minor.

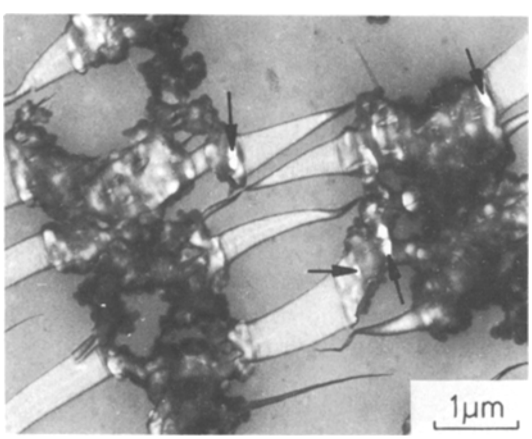

Figure 12 Typical transmission electron micrograph of crazes formed in a solvent cast film of ABS–Ib indicating the formation of voids (arrowed) at the rubber–craze interface.

The effect of graft frequency on the tensile properties of ABS–I, ABS–II, and ABS–III specimens was very similar. Increasing the graft frequency, which essentially improved the dispersion of rubber particles, resulted in an increase in yield stress and strain to failure. It was also apparent that the extent of the drop in stress on yielding was greater in materials with a high graft frequency. The microstructures observed in ultramicrotomed sections, prepared from stress whitened regions, revealed that in all cases the predominant deformation mechanism was crazing, although the variations in microstructure with

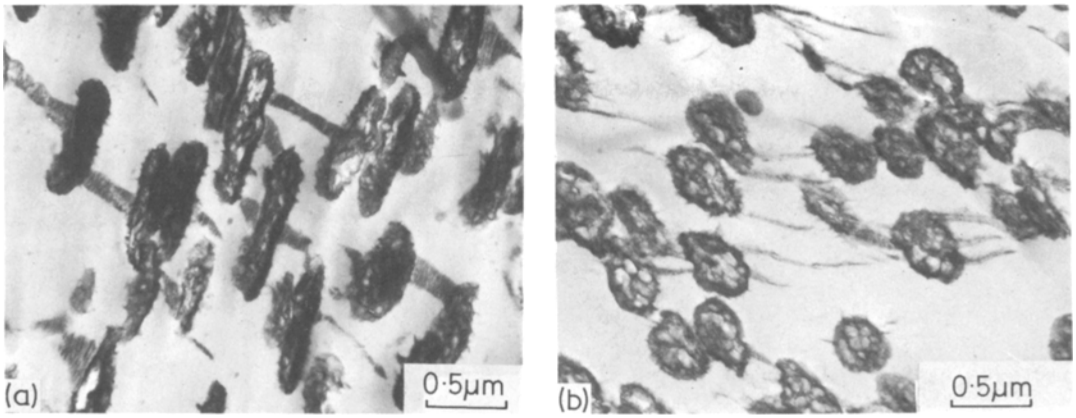

Figure 13 TEM of a microtomed section of (a) stress whitened ABS–IVa and (b) stress whitened ABS–IVd. The increased amount of occluded SAN in (b) results in an increase in the number of crazes emanating from the inclusions.

increasing graft frequency caused substantial changes in craze distribution. Crazes in ABS–Ia specimens (low graft) emanated from the agglomerated rubber regions into rubber depleted areas of the matrix and the agglomerated rubber regions were found to be highly voided. Studies of deformed cast films of ABS–I specimens with low graft frequency also indicated void formation at the rubber–matrix interface. The fracture surfaces of specimens of ABS–Ia did not contain a well-defined slow crack growth region and this suggested that crack initiation was rapidly followed by catastrophic failure. An initiation site of fracture was identified which contained a number of large voids with dimensions comparable to the diameters of the rubber agglomerations observed in ultramicrotomed sections. These observations correlate well with studies of deformation in thin sections, and the results therefore indicate that the poor mechanical properties of ABS materials with low graft frequencies are related to the irregular dispersion of weakly bonded rubber particles. The overall effect may be explained by considering that the enhanced craze formation in the vicinity of rubber particles is accompanied by de-bonding which leads to extensive voiding and premature failure.

On the other hand, ultra-thin sections prepared from stress whitened areas of specimens with higher graft frequencies contained a more uniform distribution of fine crazes, as expected due to the improved dispersion of rubber particles. In addition to this, the rubber particles in sections of ABS–Ie specimens showed no evidence of separating from the matrix despite profuse crazing in the surrounding material. Clearly then, by increasing

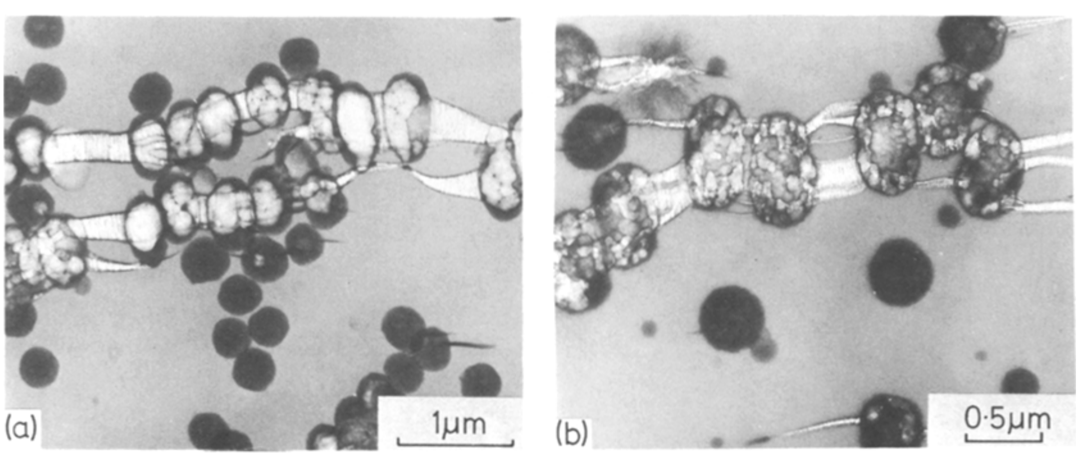

Figure 14 Typical transmission electron micrographs of crazes formed in solvent cast films of (a) ABS–IVa and (b) ABS–IVd, showing an increase in the number of crazes emanating from the rubber inclusions of specimens with increased graft frequency.

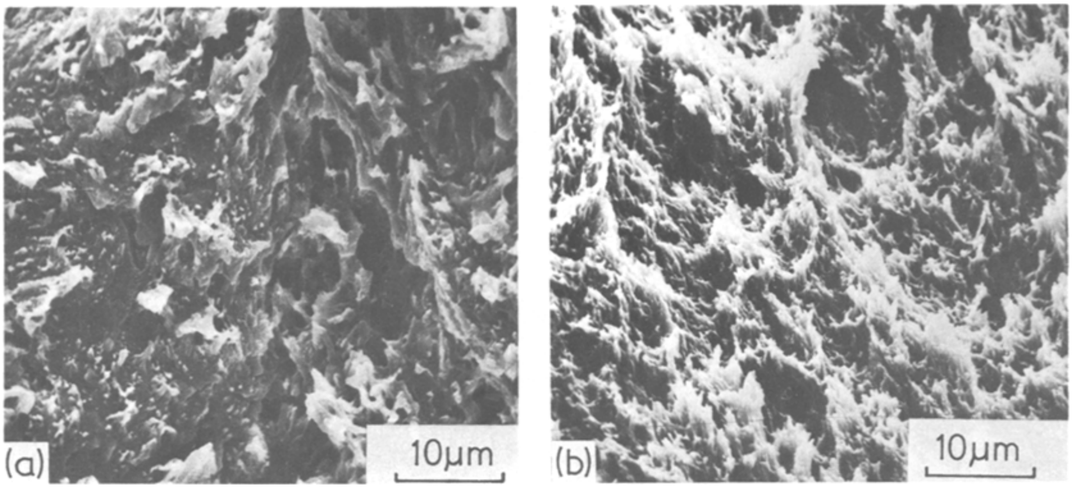

Figure 15 SEMs of (a) the initiation region of fracture in ABS–Ia indicating the presence of large voids with dimensions similar to the agglomerated rubber shown in Fig. 1a and (b) the slow growth region on the fracture surface of a specimen ABS–Ie, showing a highly drawn morphology with little indication of rubber inclusions.

the graft frequency the grafted shell of SAN becomes effective in preventing agglomeration of the rubber particles and also increases rubber–matrix adhesion. These effects combine to produce a significant improvement in mechanical properties.

The basic mechanism of rubber toughening in ABS polymers may be summarised as follows. In the early stages of a tensile test the applied load is borne mainly by the matrix and is concentrated at the equators of the rubber particles. The rubber particles act as stress concentration sites and cause the initiation of large numbers of crazes which leads to a yield point with associated stress whitening. These crazes propagate into the matrix in a direction perpendicular to the applied stress, thereby engulfing a number of rubber particles. During craze propagation, the rubber–matrix adhesion is of critical importance in sustaining triaxial tension and delaying the breakdown of crazes to produce cracks. Thus the function of rubber particles is to initiate crazes and then to stabilise the growing craze which allows further crazes to be initiated in the surrounding material. In order to toughen the brittle matrix material successfully a uniform dispersion of tightly bonded rubber particles is required. This can be achieved in the polymerisation process by ensuring that the rubber phase is adequately grafted to the matrix material.

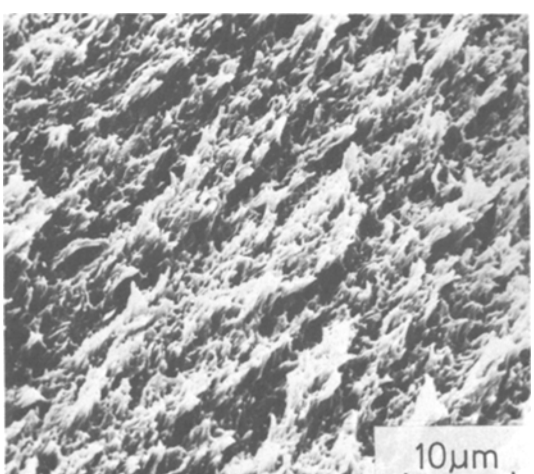

Figure 16 SEM of the slow crack growth region on the fracture surface of ABS–IVa. The fine fracture surface morphology was similar to that observed in ABS–IVa to d.

This mechanism of toughening by controlling the crazing behaviour of the matrix material, may be used to explain the observed effects of increasing graft frequency on the mechanical properties of ABS–I, –II and –III materials. For example, an irregular dispersion of weakly bonded rubber particles will be ineffective in initiating and stabilising large numbers of crazes, leading to a reduction in tensile properties. However, certain modifications to this mechanism are necessary to explain the structure–property relationship of ABS–IV materials.

The strain to failure of ABS–IV materials (average particle size = 0.4 μm) did not vary significantly and the major effect of increasing the graft frequency was found to be a small decrease in yield stress. However, the deformation mechanism characterised in ultramicrotomed sections prepared from stress whitened areas was found to vary considerably with graft frequency. A typical transmission electron micrograph of stress-whitened ABS–IVa (low graft) is shown in Fig. 13a. This micrograph clearly illustrates the ability of large rubber particles to terminate crazes, and in a number of cases some coarse crazes form between adjacent rubber particles, with little indication of craze growth continuing through the particles. It is also apparent that the particles themselves have experienced substantial elongation parallel to the tensile axis which suggests that crazing is accompanied by extensive shear deformation. This observation is in good agreement with the proposal forwarded previously that crazing and shear yielding occur simultaneously in ABS materials with little interaction, but shear yielding can only contribute significantly to the overall deformation behaviour (as indicated by substantial elongation of the inclusions) if craze growth is restricted by large rubber particles. The results of this part of the study indicate that the critical size of rubber particles which are effective in restricting craze growth is in the region of 0.26 μm and 0.41 μm, and this effect may be related to the size of inherent crazes in the matrix material. Bragaw [4] has suggested that the minimum effective particle size should be of the same order as the craze thickness or craze tip radius characteristic of the matrix polymer. Using interferometric techniques, this author estimated that crazes in a grade of SAN were approximately 0.5 to 0.6 μm thick and found that a sharp increase in the impact strength of ABS polymers occurred as the dimensions of the rubber particles exceeded this limit. In this case the effect was attributed to "craze branching".

In contrast, ultra-thin specimens of stress whitened ABS–IVd materials (high graft) showed little evidence of elongated rubber particles and the predominant deformation mechanism was attributed to crazing, although the presence of large amounts of occluded SAN caused a marked difference in the distribution of crazes. A number of crazes formed along the circumference of rubber particles and the overall craze distribution was more typical of crazing in HIPS [5]. The overall effect of differences in crazing behaviour of ABS–IV materials was to produce a reduction in yield stress with increasing graft frequency. By increasing the amount of occluded SAN, the modulus of the rubber particle increases, leading to a reduction in the stress concentration factor which should therefore increase the yield stress. On the other hand, an increase in occluded SAN results in an increase in the effective volume fraction of the dispersed phase which may cause an increase in the interaction between the stress fields of adjacent particles and thus decrease yield stress. Since the observed effect was a decrease in yield stress, this may suggest that the latter explanation is more important. An alternative explanation, forwarded by Lee [6], is that in materials containing highly occluded rubber particles, crazes may be preferentially initiated at the occlusion–rubber interface within the composite rubber particle and subsequently propagate through the matrix material.

However, the marked differences in deformation behaviour of large particle size ABS–IV materials with increasing graft frequency did not cause substantial variations in mechanical properties. Nevertheless, these results give considerable insight into the mechanism of deformation of ABS polymers in particular with respect to particle size. The contribution of shear yielding to the overall deformation behaviour appears to be related mainly with the ability of inclusions to restrict craze growth which in turn is related to the size and micromorphology of the inclusions. This mechanism differs from that proposed by Bucknall *et al.* for HIPS–PPO blends [7] in that shear in these materials involves localised areas of molecular orientation (i.e. shear bands) which are effective in controlling craze size. For ABS materials, the results suggest that the shear process is diffuse in nature and therefore rubber particles of sufficient size are necessary to control craze growth.

There is a close relationship between graft frequency and mechanical properties of ABS polymers. For ABS–I, ABS–II and ABS–III materials, which may be considered to contain solid rubber particles, increasing graft frequency causes an increase in the tensile properties. On the other hand, for ABS–IV materials increasing the graft frequency results in a small reduction in properties. In a similar study by Stabenow and Haff [2], the impact strength of a series of ABS specimens was found to pass through a maximum with increasing graft frequency although in this case a wider range of grafting than used in the present study was examined. However, it is important to note that, strictly speaking, it is not possible to relate these effects directly with grafting since a number of chemical processes occur simultaneously during polymerisation, e.g. grafting reactions, polymerisation of SAN and cross-linking of the rubber phase. It is difficult to vary these parameters independently or to analyse the effect of each process separately. Therefore a more precise view of the effect of grafting itself must await developments in the synthesis and analysis of ABS polymers.

The small quantities of model compounds available to the authors, approximately 20 g of each grade, did not provide for a systematic investigation of the effect of particle size distribution on the deformation behaviour and mechanical properties of ABS compounds. This was unfortunate because on the basis of the work described above and the work of Grancio [8, 9], the most relevant subsequent experiments would have been to select a common ABS resin (control) with a well defined small particle size (approximately 0.1 μm). This would be blended with varying fractions of ABS resins containing well defined large particles (greater than 0.4 μm) with different micromorphologies and maintained overall at a constant rubber content, this providing the basis for a systematic investigation of rubber particle size distribution and micromorphology on the mechanisms of deformation.

Acknowledgements
The authors are indebted to Borg Warner chemicals for the provision of materials and generous financial support, and to Messrs P. Beahan and J. Young for valuable advice and discussions.

The work presented in this paper was initially carried out at Liverpool University and latterly at Brunel University.

References
1. M. J. DILLON and M. BEVIS, *J. Mater. Sci.* **17** (1982) 1895.
2. J. STABENOW and F. HAF, *Ang. Makromol. Chem.* **29/30** No. 359 (1973) 1.
3. M. G. HUGUET and T. R. PAXTON, *ACS Polymer Preprints* **12** (1971) 492.
4. C. G. BRAGAW, *Adv. Chem. Ser.* **99** (1971) 86.
5. P. BEAHAN, A. THOMAS and M. BEVIS, *J. Mater. Sci.* **11** (1976) 1207.
6. D. LEE, *ibid.* **10** (1975) 661.
7. C. B. BUCKNALL, D. CLAYTON and W. E. KEAST, *ibid.* 7 (1972) 1443.
8. M. R. GRANCIO, *Polymer Eng. Sci.* **12** (1972) 213.
9. M. R. GRANCIO, A. A. BIBEAU and G. C. CLOVER, *ibid.* **12** (1972) 450.

Received 30 October
and accepted 16 November 1981